Molecular Neurobiology (2019) 56:6046–6055
https://doi.org/10.1007/s12035-019-1513-6

# Cyclooxygenase (COX) Inhibition by Acetyl Salicylic Acid (ASA) Enhances Antitumor Effects of Nitric Oxide in Glioblastoma In Vitro

Jessica Guenzle[1] · Nicklas W. C. Garrelfs[1] · Jonathan M. Goeldner[1] · Astrid Weyerbrock[1,2]

Received: 12 October 2018 / Accepted: 24 January 2019 / Published online: 4 February 2019


## Abstract

Glioblastoma multiforme (GBM) is the most aggressive brain tumor with a high recurrence rate and a median survival of about 16 months even with multimodal therapy. Novel experimental strategies against malignant gliomas include cyclooxygenase (COX) inhibition and nitric oxide (NO)–based therapies. Therapeutic doses of NO can be delivered to tumor cells by NO donors such as JS-K (O2-(2,4-dinitrophenyl)1-[(4-ethoxycarbonyl)piperazin-1-yl]diazen-1-ium-1,2-diolate) which releases NO upon enzymatic activation by glutathione S-transferase. COX-2 is frequently overexpressed in tumors and increases tumor invasiveness and angiogenesis. In this study, we show that pretreatment with acetyl salicylic acid (ASA) enhanced the cytotoxic antitumor effect of NO in vitro. Combination of low doses of JS-K and ASA revealed a dose-dependent synergistic increase of necrotic cell death under circumvention of classical apoptosis and alteration of the metabolic calcium level. These findings provide an opportunity to improve currently used therapeutic strategies in the treatment of gliomas with a well-established remedy.

**Keywords** Nitric oxide · Glioma · JS-K · Acetyl salicylic acid (ASA)

**Abbreviations**

| | |
|---|---|
| ASA | Acetyl salicylic acid |
| ATF3 | Activating transcription factor 3 |
| ATCC | American Type Culture |
| $CO_2$ | Carbon dioxide |
| DMEM | Dulbecco's modified Eagle medium |
| DMSO | Dimethyl sulfoxide |
| ECL | Enhanced chemiluminescence |
| ECM | Extracellular matrix |
| eNOS | Endothelial nitric oxide synthase |
| ETO | Etoposide |
| GAPDH | Glyceraldehyde 3-phosphate dehydrogenase |
| GBM | Glioblastoma multiforme |
| GST | Glutathione S-transferase |
| $H_2O_2$ | Hydrogen peroxide |
| iNOS | Inducible nitric oxide synthase |
| JS-K | (O2-(2,4-dinitrophenyl)1-[(4-ethoxycarbonyl)piperazin-1-yl]diazen-1-ium-1,2-diolate) |
| MTT | 3-(4,5-Dimethylthiazol-2-yl)-2,5-diphenyltetrazolium bromide |
| nNOS | Neuronal nitric oxide synthase |
| NO | Nitric oxide |
| PBS | Phosphate-buffered saline |
| PI | Propidium iodide |
| PVDF | Polyvinylidene fluoride |
| SD | Standard deviation |
| SDS | Sodium dodecyl sulfate |
| TMZ | Temozolomide |

Jessica Guenzle and Nicklas W. C. Garrelfs contributed equally to this work.

**Electronic supplementary material** The online version of this article (https://doi.org/10.1007/s12035-019-1513-6) contains supplementary material, which is available to authorized users.

✉ Astrid Weyerbrock
astrid.weyerbrock@kssg.ch

[1] Department of Neurosurgery, Medical Center, University of Freiburg, Breisacher Strasse 64, 79106 Freiburg, Germany

[2] Department of Neurosurgery, Cantonal Hospital St. Gallen, Rorschacher Strasse 95, CH-9007 St. Gallen, Switzerland

## Introduction

Glioblastoma multiforme (GBM) is the most common and aggressive brain tumor in adults, characterized by an extremely unfavorable prognosis. Despite multimodal therapy including surgery, radiotherapy, and chemotherapy, the prognosis of patients afflicted by glioblastoma remains poor with a median survival of about 16 months [1]. Since the molecular

pathogenetic mechanisms are not entirely understood yet and since gliomas appear to have intratumoral genetic heterogeneity, it is unlikely to find one successful standard therapy for this complex tumor entity. Current therapeutic advances are based on cellular mechanisms leading to activation of cell death or inhibition of tumor growth. Treatment with nitric oxide (NO) may provide a novel strategy targeting glioblastoma in recent research [2, 3]. NO is a free radical with diverse functions such as vasorelaxation, neurotransmission, and immune defense and acts as an intracellular messenger [4–7]. Endogenous NO is generated from L-arginine by NO synthases (NOS) under physiological and pathological conditions [8]. Low concentrations, induced by eNOS and nNOS, may act as cytoprotectants and promote proliferation [9]. In contrast, higher concentrations, mainly released by iNOS, may induce cell death after infiltration of macrophages into injured tissue [10]. This dual function has to be considered when using exogenous NO donors such as JS-K (O2-(2,4-dinitrophenyl)1-[4-ethoxycarbonyl)piperazin-1-yl]diazen-1-ium-1,2-diolate). The prodrug JS-K is a diazeniumdiolate that releases NO after activation by glutathione S-transferases (GSTs) which are overexpressed in glioblastoma [11, 12]. It was developed for in vitro and in vivo usage to facilitate delivery of therapeutic NO doses to target cells. In previous studies, we could demonstrate the specific release of NO by JS-K in GBM cells affecting their proliferation and cell viability in a dose- and time-dependent manner [2, 6]. Exposure to NO leads to necrotic cell death of glioma cells via mitotic catastrophe (MC) under circumvention of classical apoptosis [2]. MC is characterized by multinucleated cells with giant soma and deficiencies in cell cycle checkpoints [13, 14]. Apoptosis exhibits typical biochemical hallmarks including cleavage and activation of caspase 3 and induction of anti-apoptotic pathways. We recently demonstrated that the NO donor JS-K prevents activation of the caspase cascade by a dose-dependent activation of the anti-apoptotic Akt pathway and depletion of the intracellular ATP metabolism [2]. To improve the therapeutic benefit of NO treatment in neuro-oncology, our research has focused for the past decade on the combination of NO with chemotherapeutics, radiation, and other experimental anticancer therapeutics. In the present study, we investigated the impact of a well-studied drug on JS-K in GBM cells. The cyclooxygenase (COX) inhibitor acetyl salicylic acid (ASA) is a non-steroidal anti-inflammatory drug (NSAID) and associated with reduced risk of cancer [15, 16]. ASA is one of the most widely prescribed drugs worldwide and its effect and side effects are well characterized. In cancer research, ASA was reported to reduce the risk of cancer initiation and progression [17]. It could be shown that ASA can affect microglial activation including the ability to modulate crucial signaling pathways [18]. In GBM, it was recently reported that ASA improves the pharmacological effect of chemotherapeutics like temozolomide, bevacizumab, and sunitinib [19]. In lung cancer, ASA enhances the suppression of metastasis and promotes specific apoptosis of cancer cells by enhancing the effect of erlotinib [20]. This anti-metastatic effect is confirmed by targeting several cell functions including migration and the modulation of MMP2 [21, 22]. An RNA microarray revealed the upregulation of COX-2 expression by NO. The main objective of this study was therefore to investigate potential synergistic effect of ASA and the NO donor JS-K in GBM cells. We focused on the induction of cell death and alteration of gene expression concerning cell migration and proliferation. In this study, we provide evidence that the combination with ASA strongly enhanced the cytotoxic effect of JS-K in glioblastoma in vitro l, thus contributing to a better understanding of the therapeutic potential of NO.

## Results

### ASA Reduces Cell Viability Dose- and Time-Dependently

To investigate the impact of ASA on cell viability of the glioblastoma cell lines IC, LN229, and U87, we performed a dose-response curve using doses between 0.5 and 25 mM ASA over a treatment period of up to 48 h (Fig. 1, Suppl. S1). One hour of treatment with ASA did not reduce the cell viability of GBM cells in a significant manner whereas 48 h of exposure led to a strong reduction of viable cells starting at 0.5 mM (U87 80% ± 8%) (Suppl. S1 a–c). After 24 h, ASA decreased cell viability dose-dependently, starting at a concentration of 5 mM (U87 87% ± 2%). Cells, treated for 24 h with 10 mM ASA, showed a reduced cell population of 19% ± 6% (IC), 47% ± 4% (LN229), and 33% ± 2% (U87). To discover whether ASA enhances the dose- and time-dependent toxic effect of JS-K on GBM cells, we exposed cells for 24 h with ASA at a concentration of 10 mM for further experimental testing.

### ASA Enhances the Antitumor Effect of the NO Donor JS-K

Our group has recently studied the time- and dose-dependent effect of the NO donor JS-K over 48 h on IC, LN229, and U87 cells with concentrations up to 25 mM (1–24 h Suppl. S2A–C) [2]. In this study, ASA (10 mM, 24 h) enhanced the cytotoxic effect of JS-K after 1 h (Suppl. S2D–F), 6 h (Fig. 2a–c), and 24 h (Suppl. S2G–I) at concentrations between 1 and 15 μM dose-dependently up to 38% (LN229 6 h, 15 μM). Figure 2d reveals the enhanced cytotoxic effect of 10 mM ASA in combination with 6 h monotherapy with JS-K for each concentration up to 15 μM. ASA improved the efficacy of NO significantly between 1 and 15 μM dose- and time-dependently

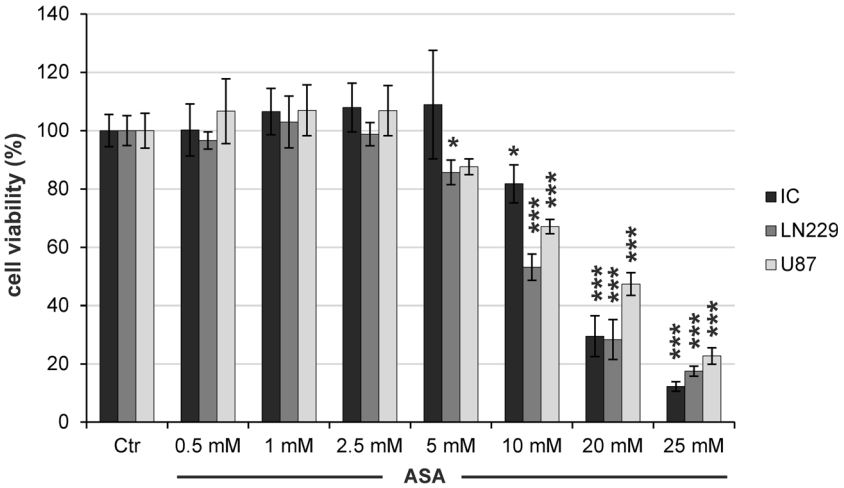


**Fig. 1** The dose-dependent cytotoxic effect of ASA (0.5–25 mM) was assessed by the MTT assay over 24 h in primary IC cells, LN229, and U87. Viability was plotted relative to untreated controls set to 100% (± S.D. of three independent experiments). Asterisks (*$P \leq 0.05$, **$P \leq 0.01$, ***$P \leq 0.001$) indicate significance compared to the control

over 24 h (Suppl. S2J–L). The calculation of the interaction index $\gamma$ revealed for IC cells $\gamma = 0.86$ at a viability of 70% ($\gamma = 10$ mM 15 mM + 5 μM 1 μM), for LN229 $\gamma = 0.8$ at a viability of 60% ($\gamma = 10$ mM 15 mM + 7 μM 1 μM), and for U87 cells $\gamma = 0.86$ at a viability of 66% ($\gamma = 10$ mM 15 mM + 5 μM 1 μM). These data reveal a synergistic effect for all cell lines when using a drug concentration of JS-K around the $IC_{50}$.

## Microarray Analysis Reveals COX-2 to Be Upregulated by NO

We determined the gene expression profile of U87 cells exposed to NO for 1 h using an RNA microarray. The data set was analyzed for altered COX-2 expression, which was 3.4-fold upregulated in a statistically significant manner ($p =$ 1.58E−07, data not shown). Subsequently, primary IC cells,

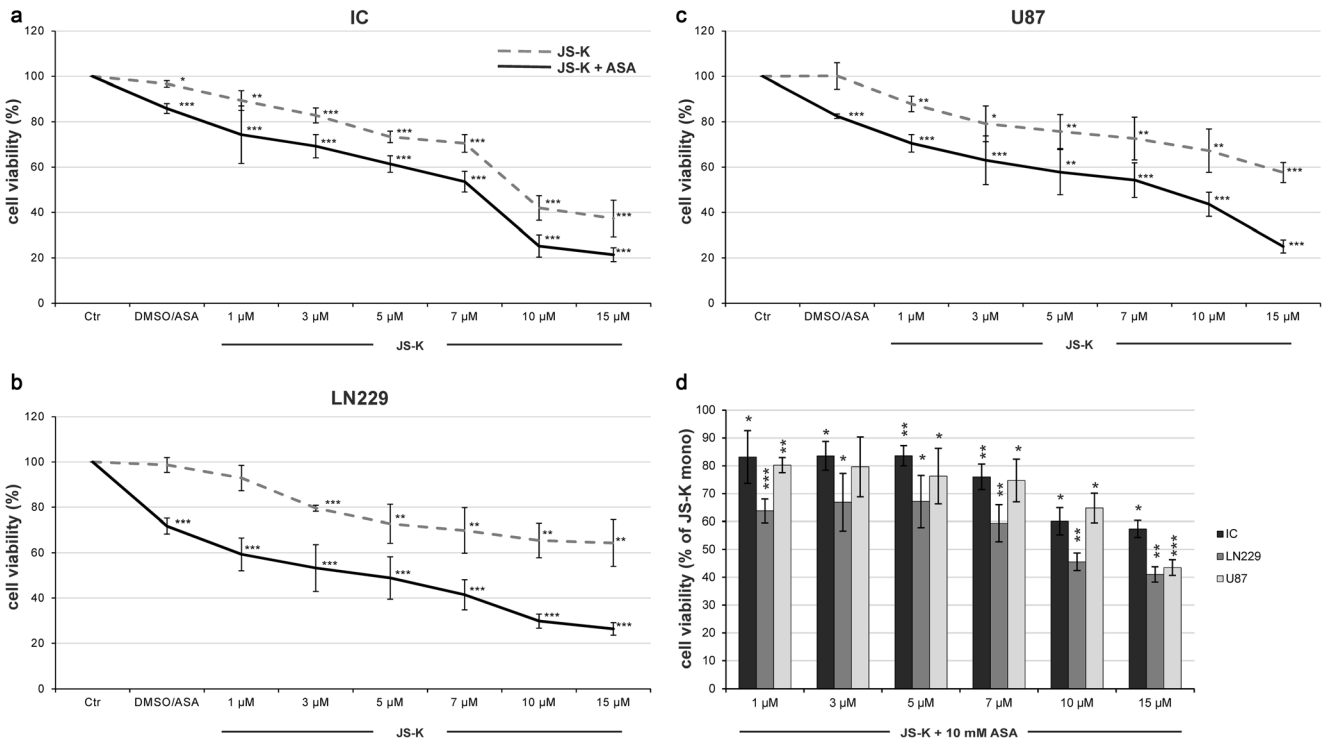


**Fig. 2** The synergistic cytotoxic effect of the combined therapy of ASA (24 h, 10 mM) and JS-K (6 h, 1–15 μM) compared to JS-K alone was determined by the MTT viability assay for primary IC cells (**a**), LN229 (**b**), and U87 (**c**). Viability was plotted relative to untreated controls set to 100%. Asterisks (*$P \leq 0.05$, **$P \leq 0.01$, ***$P \leq 0.001$) indicate significance compared to the control. Concentration of DMSO control is 0.29% according to the DMSO concentration in 15 μM JS-K. To demonstrate the efficacy compared to JS-K monotherapy (set to 100%), cell viability of combined treatment was compared to single treatment for each concentration (**d**). Asterisks (*$P \leq 0.05$, **$P \leq 0.01$, ***$P \leq 0.001$) indicate significance compared to JS-K alone. Experiments were performed in triplicates (± S.D.)

LN229, and U87 were analyzed by qRT-PCR for temporal COX-2 expression after exposure to JS-K for 6 h at concentrations up to 15 μM (Fig. 3a). All cell lines revealed a dose-dependent upregulation of COX-2 up to 17.2-fold (U87) starting at 5 μM (LN229, 6.7-fold). To investigate whether the RNA expression correlates with the actual enzyme activity, we performed a COX activity assay (Fig. 3b). The enzyme activity of COX was dose-dependently increased by JS-K after 6 h up to 10 μM. LN229 achieved a twofold upregulation compared to controls ($p = 0.02$), whereas ASA alone did not change COX enzyme activity (n.s.).

## Combined Therapy of ASA and NO Leads to Altered Gene Expression

In previous studies, we showed that JS-K alters the gene expression of several genes involved in the regulation of migration, invasion, and proliferation [23]. Combined treatment with JS-K and ASA showed increased RNA expression levels of ATF3 (activating transcription factor 3), EGR1 (early growth response 1), and EGR2 (early growth response 2) compared to monotherapy with JS-K (Fig. 4a–c). The expression level of ATF3 in LN229 cells exposed to JS-K and ASA was upregulated 22-fold compared to JS-K monotherapy from 1.6 to 36.2-fold expression (Fig. 4a). ATF3 regulates the expression and activity of matrix metalloproteinases and tissue inhibitors of matrix metalloproteinases and thereby the migration and invasion ability of GBM cells in vitro [23]. The expression level of EGR1 was upregulated 24.8-fold in primary IC cells compared to JS-K alone, whereas JS-K downregulated the investigated gene twofold (Fig. 4b). The transcription factor EGR1 is involved in migration processes by regulation of extracellular matrix proteins and growth factors and has antiproliferative properties. The expression level of EGR2 was upregulated 28.6-fold in primary IC cells compared to JS-K monotherapy, whereas JS-K did not alter the expression of EGR2 (0.8-fold). EGR2 is associated with proliferation of lymphocytes in humans.

## COX Inhibition Enhances Necrosis Induced by NO

JS-K was identified to induce cGMP-dependent necrotic cell death in primary and immortalized GBM cell line [2]. Flow cytometry of cells exposed to both ASA and JS-K revealed an expansion of the necrotic cell population to more than 70% by ASA compared to JS-K alone (Fig. 5a, IC, 10 μM JS-K). Cell numbers in the apoptotic cell population remained nearly stable under 10% for all cell lines and were not altered by ASA (Fig. 5). To exclude the involvement of caspase-dependent apoptosis, we analyzed the activation of caspase 3 (c-casp 3) by Western blot analysis (Fig. 6a). Neither JS-K alone (10 μM for 6 h) nor the combination with 10 mM ASA activated caspase 3 by cleavage to the fragment size of 17 kDa or other. Since cleavage of caspase 3 can also be detected by a decrease of the pro-caspase, we performed a Western blot analysis for full-length pro-caspase 3, but no decrease could be observed at 35 kDa (Suppl. S3). Classical apoptosis can be regulated by the anti-apoptotic Akt pathway. Western blot analysis of Akt and activated, i.e., phosphorylated, Akt (p-Akt) demonstrated a dose-dependent decrease of Akt in primary IC cells (Fig. 6b). However, the protein level of activated Akt is dose-dependently enhanced by exposure to NO. The combined treatment with JS-K (1–10 μM) and ASA (10 mM) led to an increase of activated Akt compared to monotherapy with JS-K. However, the protein level of Akt is even more decreased than with JS-K monotherapy. This demonstrates that COX inhibition enhances the anti-apoptotic effect of NO on GBM cells. Calcium triggers key cellular functions, but an overload of $Ca^{2+}$ is toxic for cells [24]. A strong $Ca^{2+}$ influx causes mitochondrial damage and a collapse of the mitochondrial membrane potential ($\Delta\Psi_m$) [25]. Monotherapy with JS-K increased the intracellular $Ca^{2+}$ concentration in primary IC cells to 195% (± 8%). This finding supports the assumption of necrotic cell death in GBM cells (Fig. 6c). The combination with ASA enhanced the intracellular $Ca^{2+}$ level to more than 300% (± 31%) compared to controls. Figure 6 d–g show representative images of the $Ca^{2+}$ concentration visualized by

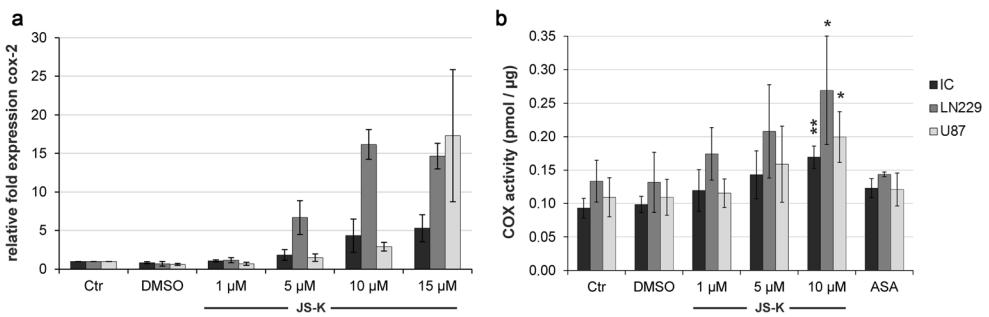


**Fig. 3** All cells lines revealed dose-dependent relative fold expression of COX-2 induced by JS-K treatment up to 15 μM over 6 h (**a**). Data of qRT-PCR show mean ± S.D. of triplicates normalized to untreated controls set to 1. Enzyme activity of COX-2 (**b**) was determined by peroxidase assay for IC cells, LN229, and U87. Activity (pmol/μg total protein) of DMSO controls, JS-K-treated cells (1–10 μM, 6 h) and ASA (10 mM, 24 h)-treated cells were normalized to untreated controls ± S.D. of triplicate. Asterisks (*$P \le 0.05$, **$P \le 0.01$, ***$P \le 0.001$) indicate significance compared to control

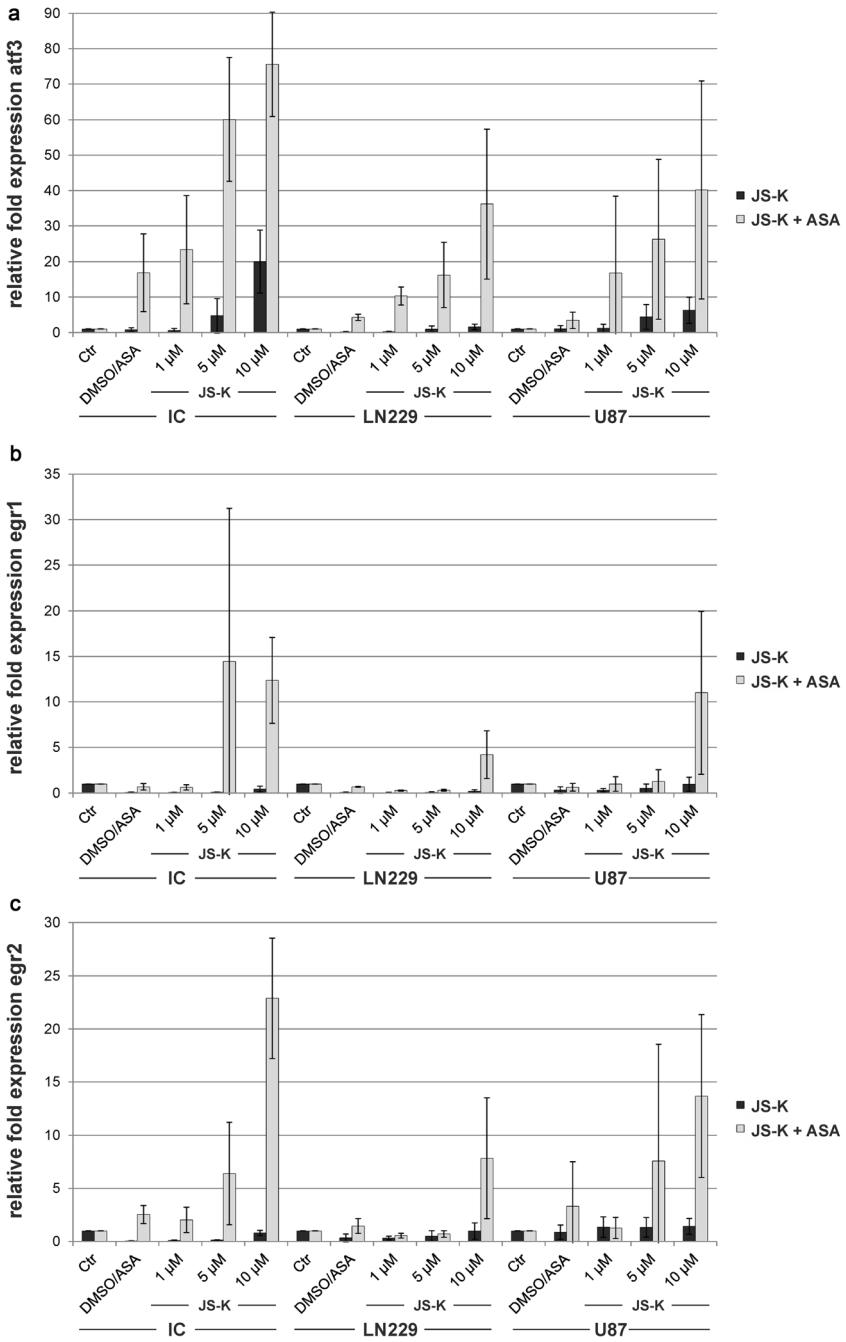


**Fig. 4** Relative fold expression of *atf3* (**a**), *egr1* (**b**), and *egr2* (**c**) was assessed by qRT-PCR for primary IC cells, LN229, and U87. Dose-dependent induction of gene expression by JS-K (6 h, 1–10 μM) was enhanced by combination with ASA (24 h, 10 mM). The DMSO/ASA control shows the DMSO control as solvent of JS-K (black) and the ASA monotherapy (gray). Data of qRT-PCR show mean ± S.D. of triplicates normalized to untreated controls set to 1

fluorescence microscopy. Images reveal decreased cell numbers according to the cytotoxic effect of JS-K and ASA. Data were normalized to controls according to the total cell number in MTT assay.

## Discussion

Cyclooxygenases are known to be responsible for the formation of thromboxane and prostaglandins, mediators of vasoconstriction and inflammation. The inducible synthases are associated with tumor angiogenesis [26] and malignancy in various cancers [27]. COX expression also correlates with overall survival and chemoresistance of GBM patients [28]. In previous studies, inhibition of COX resulted in a reduction of angiogenesis and glioma growth [29]. COX inhibitors have been shown to exert a synergistic antitumor and anti-angiogenic effect in combination with radiation in vivo [30, 31]. Since glioblastoma is the most aggressive brain tumor in humans with a dismal prognosis, new strategies for GBM treatment are required. We recently published several experimental studies concerning the use of the NO donor JS-K in

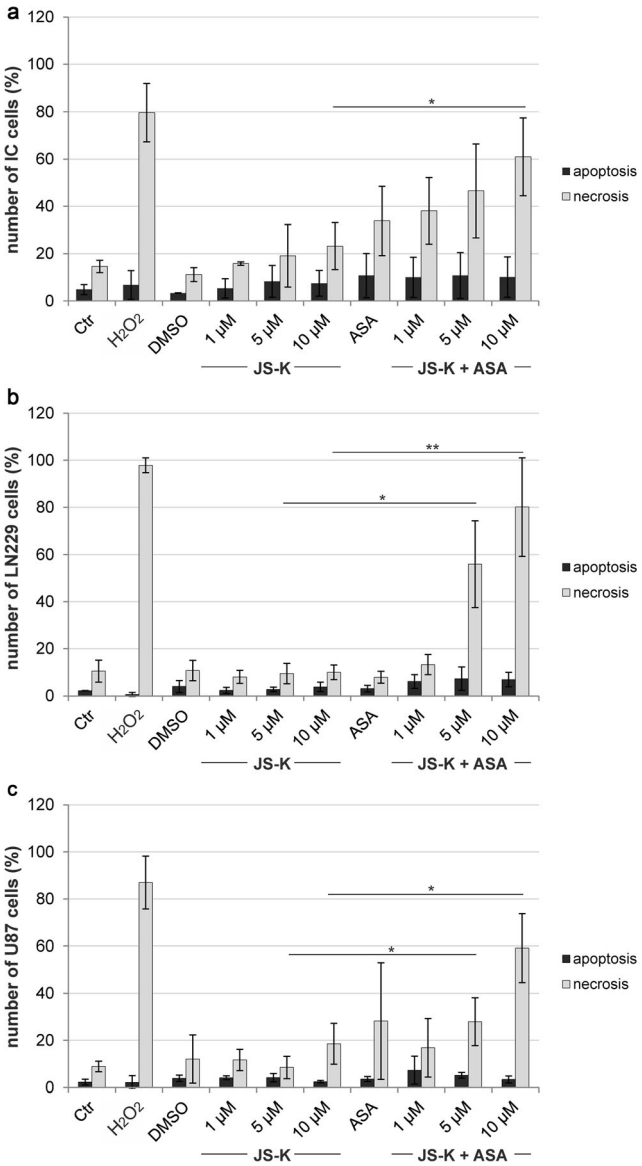


**Fig. 5** To demonstrate the dose-dependent enhancement of necrotic cell populations by ASA (24 h, 10 mM) compared to JS-K monotherapy (6 h, 1–10 μM), flow cytometry analysis of annexin V and PI was performed for primary IC cells (**a**), LN229 (**b**), and U87 (**c**). DMSO controls according to 10 μM JS-K (0.19%) and necrosis inducing control (3 mM $H_2O_2$) were performed. Treatment groups were normalized to total cell number and plotted relative to untreated controls ± S.D. Asterisks (*$P \leq 0.05$, **$P \leq 0.01$, ***$P \leq 0.001$) indicate significance of combined treatment compared to JS-K alone

gliomas [6, 11]. JS-K releases NO after enzymatic metabolization by glutathione S-transferases. Exposure of GBM cells to NO has dichotomous effects. High concentrations up to 25 μM JS-K resulted in mitotic catastrophe leading to necrotic cell death whereas lower concentration up to 3 μM led to reduced invasion and migration by upregulation of the transcription factor ATF3 [2, 23]. NO and its metabolite peroxynitrite bind to the iron-heme center in the active site of COX and therefore enhance the activity of the synthase [32, 33] as demonstrated by COX activity assay. Kim et al. demonstrated in murine macrophages that NO mediates S-nitrosylation of cysteine residues of COX-2 leading to a strong activation [33]. Additionally, the mitochondrial dysfunction caused by JS-K induces COX expression and storage of COX-2 in the mitochondria [34]. COX inhibition interrupts this process of regeneration and renewal. The COX inhibitor ASA is known for its antiproliferative and apoptotic effect in several tumors [35, 36]. Therefore, combining COX inhibitors and NO appears to be a promising antitumor strategy. In the present work, we demonstrated the synergistic effect of ASA on JS-K treatment in GBM cells. While JS-K leads to necrotic cell death and metabolic changes, ASA enhances these anti-tumor effects significantly and alters the gene expression of the cells. The synergistic effect of the combination of two different medications can be calculated by an isobole-based statistical model [37]. In this work, we present the interaction index $\gamma \sim 0.8$ which demonstrates the advantage of the combination of NO and ASA. High concentrations of both compounds may be associated with severe side effects. Combining both agents allows reduction of the doses without reduction of efficacy. Inhibition of COX-2 enhanced the sensitivity of the GBM cells to cytotoxic agents such as NO. This is in line with findings of Xu et al. showing that the expression level of COX-2 correlates with the grade of resistance on GBM cells [28]. Resistance mechanisms are related to gene expression alterations in many cases. The transcription factor EGR2 is a key regulator of the immune response and a negative regulator of COX-2 [38]. The expression of EGR2 was significantly upregulated by the combination of NO and ASA whereas the monotherapy of each did not influence gene expression. This synergistic effect might lead to the enhanced induction of cell death. EGR2 is known to induce apoptosis in various cancer cells by inhibition of anti-apoptotic mechanisms such as the Akt pathway [39]. We found Akt signaling to be dose-dependently upregulated by JS-K and enhanced by ASA. At the same time, egr2 is downregulated. In contrast to the findings of Unoki et al., the upregulation of egr2 did not induce classical apoptosis in GBM cells. In previous studies, we found that exposure to NO induces mitotic catastrophe in GBM cells leading to necrotic cell death. This effect was synergistically enhanced by the combination of ASA in this study. Classical apoptosis was excluded by the absence of cleaved caspase 3 and an apoptotic population in flow cytometry analysis. The transcription factor EGR1 (early growth response protein 1) is involved in the regulation of proliferation and differentiation [40]. In endothelial cells, EGR1 is regulated by iNOS and NO [41]. In the present work, we confirm the dose-dependent upregulation of EGR1 in GBM cells by high concentrations of the NO donor JS-K. Although ASA alone has no influence on gene expression of egr1, it enhances the upregulation induced by JS-K synergistically. The stress-induced upregulation of EGR1 is a very fast transient process

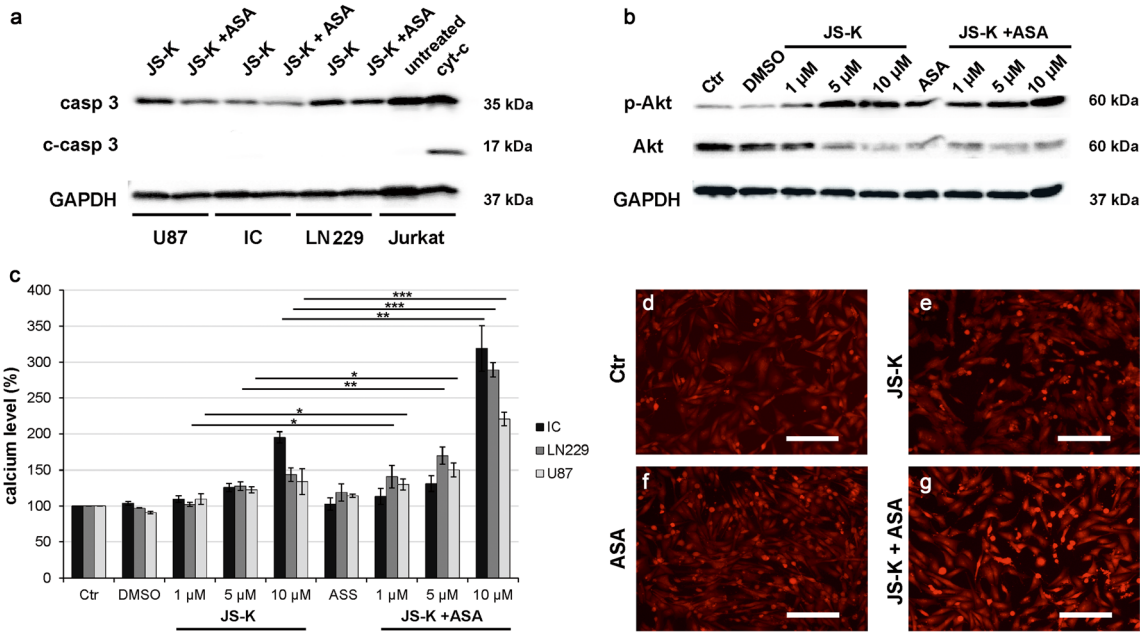


**Fig. 6** Representative Western Blot analysis of pro-caspase 3 (35 kDa) and activated caspase 3 (c-casp 3, 17 kDa) indicates no influence of JS-K (10 μM, 6 h) and ASA (10 mM, 24 h) on classical apoptosis (**a**) in primary IC cells, LN229, and U87. Untreated as well as cytochrome c–treated (cyt-c) Jurkat cells were used as negative and positive controls. The dose-dependent activation of the anti-apoptotic Akt signaling as well as the reduction of non-phosphorylated Akt (60 kDa) induced by JS-K (6 h, 1–10 μM) was enhanced by ASA (24 h, 10 mM) in LN229 (**b**). DMSO had no influence on protein expression and activation. 25 μg of protein lysates were separated by SDS-PAGE in three independent experiments. GAPDH was used as loading control. Intracellular calcium levels of primary IC cells, LN229, and U87 induced by JS-K (6 h, 1–10 μM) alone and the combination with ASA (24 h, 10 mM) were determined by calcium mobilization assay (**c**). Treatment and DMSO controls were normalized to untreated controls set to 100%. Asterisks (*$P \leq 0.05$, **$P \leq 0.01$, ***$P \leq 0.001$) indicate significance to controls; experiments were performed in triplicates. Representative images of intracellular calcium in primary IC cells pre-loaded with Rhod-4 (red) show the synergistic effect of the combined treatment of JS-K and ASA (**g**) compared to single treatment with JS-K (**e**, 5 μM, 6 h) or ASA (**f**, 10 mM, 24 h) as well as the controls (**d**). Samples were analyzed by microscopy (× 10, scale bar represents 100 μm)

which disappears again within hours. Giraldo et al. found the transcription factor ATF3 as a negative regulator of EGR1 [42]. In our work, we demonstrate a dose-dependent upregulation of atf3 with the combination of ASA and NO. The presence of ATF3 might be a reason for the fast reduction of egr1. In contrast to NO, ASA alone upregulated the expression of atf3 significantly. Therefore, we conclude that JS-K enhances the effect of the COX inhibitor. ATF3 was recently shown to reduce the migration and invasion ability of GBM cells by inhibiting NFκB and STAT3 activation [23]. STAT3 in turn regulates the kinetics of cellular metabolism [43]. We recently demonstrated that NO decreases intracellular ATP levels [2]. ASA is also known to reduce intracellular ATP levels by unbalanced electron transport in the mitochondria [44]. This mitochondrial dysfunction leads to unrestrained efflux of calcium ions into the cytosol. The usual exchange of calcium ions is mediated by transporters such as the VDAC (voltage-dependent anion channel) or the PTP (permeability transition pore) in the membrane of mitochondria and the endoplasmic reticulum [45]. ASA induces a permanent efflux of $Ca^{2+}$ into the cytosol through these transporters that usually leads to apoptotic cell death [36, 46]. Classical apoptosis requires plenty of energy in the form of ATP for protein expression and enzymatic activity for DNA repair and maintenance of cell integrity [47, 48]. The dose-dependent decrease of ATP inevitably leads to necrotic cells death as shown by FACS analysis of NO- and ASA-treated cells. The combination again resulted in increased induction of necrosis. As ASA inhibits the reflux of $Ca^{2+}$ in the mitochondria and the ER by blocking the PTP, necrosis can no longer be prevented. These obvious changes in the metabolic system of the GBM cells are induced by the synergistic effect of NO combined with ASA. Future research effort should focus on maximizing the treatment effect of cancer drugs while reducing side effects in the treatment of patients. The results of this study provide further insight into the therapeutic potential of NO in glioblastoma treatment in combination with ASA as a sensitizing agent.

## Materials and Methods

### Cell Culture

Established human glioma cell lines U87MG and LN229 (ATCC, Manassas, USA) as well as the primary glioblastoma cell line IC were cultured in Dulbecco's modified Eagle medium (DMEM) containing 10% fetal bovine serum and 1%

penicillin/streptomycin at 37 °C in a humidified atmosphere containing 5% $CO_2$. The primary cell line IC was established from a surgical specimen of a patient with glioblastoma multiforme. Retrieval and scientific analysis of patient-derived tissue was approved by the local ethics committee under protocol 100020/09. The NO donor JS-K [O2-(2,4-dinitrophenyl)1[(4-ethoxycarbonyl)piperazin-1-yl]diazen-1-ium-1,2-diolate] was synthesized as described earlier [49]. Cells were exposed to JS-K concentrations between 1 and 25 μM (stock solution 5.2 mM in DMSO) or ASA between 0.5 and 25 μM (stock solution 550 mM in $H_2O$) for up to 48 h when they reached 70–80% confluence. The final concentration of DMSO was not higher than 0.05% (when using 25 μM JS-K).

## MTT Assay

Cell viability was determined by the MTT assay. $10^4$ cells were grown in 96-well plates with complete DMEM. Cells were treated with either 0.5–25 mM ASA for 1–48 h or 1–25 μM JS-K for 24 h or in combination. The MTT assay was performed as described before [11]. Absorbance at 570 nm was measured with Tecan Infinite200 (Tecan, Männedorf, Switzerland). Percentages were calculated relative to the viability of untreated controls or to JS-K monotherapy set to 100%.

## Calculation of the Synergistic Index

The synergistic effect is the superadditive of two combined treatments, whereas the overall effect is more than the sum of the single effects. The synergistic index was calculated using the interaction index $\gamma$ [50]. The calculation of the interaction index $\gamma$ is derived from an isobole-based statistical model [37]. $\gamma = a/A + b/B$, if $a = c$ (ASA in combination with JS-K); $b = c$ (JS-K in combination with ASA); $A = c$ (ASA alone); $B = c$ (JS-K alone) for a constant viability. The easiest model is that of the additional effect if $a/A + b/B = 1$. The following possibilities arise: $\gamma = 1$, additive effect; $\gamma > 1$, subadditive effect (antagonistic); $\gamma < 1$, superadditive effect (synergistic).

## Microarray

Gene expression changes were investigated by microarray using the Illumina HumanHT-12 Expression BeadChip for analysis of 31,000 genes. The array was performed at the German Cancer Research Center (DKFZ), Heidelberg, Germany. RNA samples were purified from U87 treated with 15 μM JS-K for 1 h as well as from untreated controls. Gene upregulation caused by JS-K was evaluated. Microarray was done in triplicate.

## RNA Purification and qRT-PCR

Total RNA was prepared from U87, LN229, and IC cells using the RNeasy mini kit according to the manufacturer's instructions (Qiagen, Hilden, Germany). cDNA was generated from 1 μg of total RNA in a volume of 30 μl using M-MuLV reverse transcriptase (Thermo Scientific, USA) and 100 pmol of hexameric primers. cDNA was quantified by quantitative real-time PCR on a StepOnePlus™ System (Thermo Scientific, USA) using SYBR™ Green Master Mix (Thermo Scientific, USA) and specific primers for COX-2 (Qiagen, Hilden, Germany), ATF3 (5′-CCTCTGCGCTGGAATCAGTC-3′ forward; 5′-TTCTTTCTCGTCGCCTCTTTTT-3′ reverse), EGR1 (5′-ACCGCAGAGTCTTTTCCTGA-3′ forward; 5′-CTCACTAGGCCACTGACCAA-3′ reverse), EGR2 (5′-GGTGACCATCTTTCCCAATG-3′ forward; 5′-TGGGATATGGGAGATCCAAC-3′ reverse), and RPS18 (5′-TTTTGCGAGTACTCAACACCA-3′ forward; 5′-CCACACCCCTTAATGGCA-3′ reverse) as endogenous control. The conditions were 95 °C for 20 s, followed by 40 cycles of 3 s at 95 °C, and 30 s at 60 °C. The relative expression level of the target gene compared with that of the housekeeping gene RPS18 was calculated with the $2^{-\Delta\Delta Ct}$ method and normalized to the untreated control set to 1.

## COX Activity Assay

$5 \times 10^5$ cells were cultured in complete DMEM and treated with JS-K (1–10 μM) for 6 h or ASA (10 mM) for 24 h. Cells were harvested and lysed with 1% igepal/PBS (Sigma-Aldrich, Munich, Germany). COX assay was performed according to the manufacturer's protocol (COX Activity Assay Kit Fluorimetric, Abcam ab204699, Cambridge, UK). Absorption at 535 nm (reference 587 nm) was measured with Tecan Infinite200 (Tecan, Männedorf, Switzerland). The total amount of COX activity (pmol/μg) per 5 μl sample was calculated according to the standard curve and the concentration of total protein. Lysates of untreated and DMSO-treated cells were included as controls.

## Flow Cytometry

Flow cytometry was performed to distinguish between apoptosis and necrosis with annexin V (Life Technologies Alexa Fluor 647 #23204) and propidium iodide (PI) as described before with FACS Calibur (Beckman Coulter, Brea, CA, USA) [2]. $10^5$ cells were exposed to 1–10 μM JS-K for 6 h and 10 mM ASA for 24 h. Populations were analyzed using the FlowJo Diagnostic software (FlowJo, LLC, OR, USA).

### Western Blotting

Glioma cells were cultured in complete DMEM. Equal amounts of protein (20 μg of lysate) were applied on 10% SDS-polyacrylamide gels and electrophoresed (BioRad, Munich, Germany). Proteins were blotted on PVDF membranes by wet blotting (BioRad, Munich, Germany). Epitopes were blocked with 5% non-fat milk in Tris-buffered saline with 0.05% Tween20 (MP/TBST) for 1 h at room temperature (RT). Blots were incubated with primary antibodies anti-caspase 3 (rabbit, #9662, 1:1000, Cell Signaling Technology, Inc., Boston, USA), anti-cleaved caspase 3 (rabbit, #9915, 1:1000, Cell Signaling Technology, Inc., Boston, USA), anti-p-Akt (Serin473) (rabbit, 1:1000, Cell Signaling Technology, Inc., Boston, USA), anti-Akt (goat, sc-1619, 1:1000, Santa Cruz Biotechnology, Santa Cruz, CA, USA), and anti-GAPDH (mouse, 1:10000 Abcam, Cambridge, UK) overnight at 4 °C in 5% MP/TBST. After incubation with secondary antibodies goat anti-rabbit/mouse and rabbit anti-goat (Santa Cruz Biotechnology, Santa Cruz, CA, USA) for 1 h at RT, proteins were visualized by enhanced chemiluminescence (BioRad, Munich, Germany). Jurkat cell and cytochrome c–treated Jurkat cells were used as controls for apoptosis. GAPDH was used as loading control.

### Evaluation of the Intracellular Calcium Concentration

According to the supplier's protocol, $10^4$ cells were cultured on 96-well plates in complete DMEM. Cells were exposed to 1–10 μM JS-K for 6 h and 10 mM ASA for 24 h. 100 μl Rhod-4 dye-loading solution was added to the cells and incubated for 30 min at 37 °C and for 30 min at RT. Absorbance at 540 nm (reference 590 nm) was measured with Tecan Infinite200 (Tecan, Männedorf, Switzerland). Percentages were calculated relative to the viability of untreated controls or to JS-K monotherapy set to 100%. Additionally, fluorescence was visualized by microscopy (× 10, Zeiss Axio Observer). Scale bars represent 100 μm.

### Statistical Analysis

All experiments were performed in triplicates. Data are shown as mean ± SD. Data were compared using an unpaired two-tailed Student's $t$ test; $P < 0.05$ was considered statistically significant.

### Compliance with Ethical Standards

**Conflict of Interest** The authors declare that they have no competing interests.



## References

1. Stupp R et al (2005) Radiotherapy plus concomitant and adjuvant temozolomide for glioblastoma. N Engl J Med, Bd 352(Nr. 10): 987–996
2. Günzle J, Osterberg N, Saavedra JE, Weyerbrock A (2016) Nitric oxide released from JS-K induces cell death by mitotic catastrophe as part of necrosis in glioblastoma multiforme. Cell Death Dis, Bd 7(Nr. 9):e2349
3. Weidensteiner C et al (2013) Effects of the nitric oxide donor JS-K on the blood-tumor barrier and on orthotopic U87 rat gliomas assessed by MRI. Nitric Oxide, Bd 30:17–25
4. Garthwaite J (2008) Concepts of neural nitric oxide-mediated transmission. Eur J Neurosci, Bd 27(Nr. 11):2783–2802
5. Weyerbrock A, Walbridge S, Saavedra JE, Keefer LK, Oldfield EH (2011) Differential effects of nitric oxide on blood-brain barrier integrity and cerebral blood flow in intracerebral C6 gliomas. Neuro Oncol, Bd 13(Nr. 2):203–211
6. Kogias E et al (2012) Growth-inhibitory and chemosensitizing effects of the glutathione-S-transferase-π activated nitric oxide donor PABA/NO in malignant gliomas. Int J Cancer, Bd 1(Nr. 1305): 1184–1194
7. Shami PJ et al (Nov. 2009) JS-K, An arylating nitric oxide (NO) donor, has synergistic anti-leukemic activity with cytarabine (ARA-C). Leuk Res, Bd 33(Nr. 11):1525–1529
8. Ignarro LJ (1990) Biosynthesis and metabolism of endothelium-derived nitric oxide. Annu Rev Pharmacol Toxicol, Bd 30(Nr. 8): 535–560
9. Contestabile A, Ciani E (2004) Role of nitric oxide in the regulation of neuronal proliferation, survival and differentiation. Neurochem Int, Bd 45(Nr. 6):903–914
10. Fitzpatrick B, Mehibel M, Cowen RL, Stratford IJ (2008) iNOS as a therapeutic target for treatment of human tumors. Nitric Oxide, Bd 19(Nr. 2):217–224
11. Weyerbrock A et al (2011) JS-K, a glutathione S-transferase-activated nitric oxide donor with antineoplastic activity in malignant gliomas. Neurosurgery, Bd 70(Nr. 2):497–510
12. Shami PJ et al (2003) Nitric oxide donor of the diazeniumdiolate class with potent antineoplastic activity 1. Mol Cancer Ther, Bd 2(Nr. April):409–417
13. Roninson IB, Broude EV, Chang B-D (2001) If not apoptosis, then what? Treatment-induced senescence and mitotic catastrophe in tumor cells. Drug Resist Updat, Bd 4(Nr. 5):303–313
14. Hung J et al (2013) Subamolide A induces mitotic catastrophe accompanied by apoptosis in human lung cancer cells, Evidence-Based Complement. Altern Med, Bd 2013. https://doi.org/10.1155/2013/828143
15. Cho M et al (2013) Aspirin blocks EGF-stimulated cell viability in a COX-1 dependent manner in ovarian cancer cells. J Cancer, Bd 4(Nr. 8):671–678
16. Nath N, Vassell R, Chattopadhyay M, Kogan M, Kashfi K (2009) Nitro-aspirin inhibits MCF-7 breast cancer cell growth: effects on COX-2 expression and Wnt/ß-catenin/TCF-4 signaling. Biochem Pharmacol, Bd 78(Nr. 10):1298–1304
17. Rothwell PM, Wilson M, Price JF, Belch JF, Meade TW, Mehta Z (2012) Effect of daily aspirin on risk of cancer metastasis: a study of incident cancers during randomised controlled trials. Lancet, Bd 379(Nr. 9826):1591–1601
18. Ajmone-Cat MA, Bernardo A, Greco A, Minghetti L (2010) Non-steroidal anti-inflammatory drugs and brain inflammation: effects on microglial functions. Pharmaceuticals, Bd 3(Nr. 6):1949–1964

19. Navone SE et al (2018) Aspirin affects tumor angiogenesis and sensitizes human glioblastoma endothelial cells to temozolomide, bevacizumab, and sunitinib, impairing vascular endothelial growth factor-related signaling. World Neurosurg, Bd 120:e380–e391
20. Hu X, Wu L-W, Weng X, Lin N-M, Zhang u C (2018) Synergistic antitumor activity of aspirin and erlotinib: inhibition of p38 enhanced aspirin plus erlotinib-induced suppression of metastasis and promoted cancer cell apoptosis. Oncol Lett, Bd 16(Nr. 2): 2715–2724
21. Guillem-Llobat P et al (2016) Aspirin prevents colorectal cancer metastasis in mice by splitting the crosstalk between platelets and tumor cells. Oncotarget, Bd 7(Nr. 22):32462–32477
22. Khan P et al (2016) Aspirin inhibits epithelial-to-mesenchymal transition and migration of oncogenic K-ras-expressing non-small cell lung carcinoma cells by down-regulating E-cadherin repressor slug. BMC Cancer, Bd 16(Nr. 1):39
23. Guenzle J et al (2017) ATF3 reduces migration capacity by regulation of matrix metalloproteinases via NFκB and STAT3 inhibition in glioblastoma. Cell Death Discov, Bd 3(Nr. December 2016): 17006
24. Duchen MR (2000) Mitochondria and calcium: from cell signalling to cell death. J Physiol, Bd 529(Pt 1, Nr April):57–68
25. Jambrina E et al (2003) Calcium influx through receptor-operated channel induces mitochondria-triggered paraptotic cell death. J Biol Chem, Bd 278(Nr. 16):14134–14145
26. Masferrer JL et al (2000) Antiangiogenic and antitumor activities of cyclooxygenase-2 inhibitors. Cancer Res, Bd 60:1306–1311
27. Ferrandina G et al (2002) Increased cyclooxygenase-2 (COX-2) expression is associated with chemotherapy resistance and outcome in ovarian cancer patients. Ann Oncol, Bd 13(Nr. 8):1205–1211
28. Xu K, Wang L, Shu H-KG (2014) COX-2 overexpression increases malignant potential of human glioma cells through Id1. Oncotarget, Bd 5(Nr. 5):1241–1252
29. Leahy KM, Ornberg RL, Wang Y, Zweifel BS, Koki AT, Masferrer JL (2002) Cyclooxygenase-2 inhibition by celecoxib reduces proliferation and induces apoptosis in angiogenic endothelial cells in vivo advances in brief cyclooxygenase-2 inhibition by celecoxib reduces proliferation and induces apoptosis in angiogenic endothelial C. Cancer Res, Bd 62(Nr. 3):625–631
30. Wagemakers M et al (2009) COX-2 inhibition combined with radiation reduces orthotopic glioma outgrowth by targeting the tumor vasculature. Transl Oncol, Bd 2(Nr. 1):1–7
31. Petersen C et al (2000) Enhancement of intrinsic tumor cell radiosensitivity induced by a selective cyclooxygenase-2 inhibitor enhancement of intrinsic tumor cell radiosensitivity induced by a selective cyclooxygenase-2 inhibitor. Clin Cancer Res, Bd 6(Nr. June):2513–2520
32. Salvemini D, Misko TP, Masferrer JL, Seibert K, Currie MG, Needleman P (1993) Nitric oxide activates cyclooxygenase enzymes. Proc Natl Acad Sci U S A, Bd 90(Nr. 15):7240–7244
33. Kim SF (2005) Inducible nitric oxide synthase binds S-nitrosylates, and activates cyclooxygenase-2. Science, Bd (80) 310(Nr. 5756): 1966–1970
34. Cillero-Pastor B, Caramés B, Lires-Deán M, Vaamonde-García C, Blanco FJ, López-Armada MJ (2008) Mitochondrial dysfunction activates cyclooxygenase 2 expression in cultured normal human chondrocytes. Arthritis Rheum, Bd 58(Nr. 8):2409–2419
35. Lai MY, Huang JA, Liang ZH, Jiang HX, Tang GD (2008) Mechanisms underlying aspirin-mediated growth inhibition and apoptosis induction of cyclooxygenase-2 negative colon cancer cell line SW480. World J Gastroenterol, Bd 14(Nr. 26):4227–4233
36. Kern MA et al (2006) Cyclooxygenase-2 inhibition induces apoptosis signaling via death receptors and mitochondria in hepatocellular carcinoma. Cancer Res, Bd 66(Nr. 14):7059–7066
37. Sørensen H, Cedergreen N, Skovgaard IM, Streibig JC (2007) An isobole-based statistical model and test for synergism/antagonism in binary mixture toxicity experiments. Environ Ecol Stat, Bd 14(Nr. 4):383–397
38. Barbeau DJ, La KT, Kim DS, Kerpedjieva SS, Shurin GV, Tamama K (2014) Early growth response-2 signaling mediates immunomodulatory effects of human multipotential stromal cells. Stem Cells Dev, Bd 23(Nr. 2):155–166
39. Unoki M, Nakamura Y (2003) EGR2 induces apoptosis in various cancer cell lines by direct transactivation of BNIP3L and BAK. Oncogene, Bd 22(Nr. 14):2172–2185
40. Myung DS et al (2014) Expression of early growth response-1 in colorectal cancer and its relation to tumor cell proliferation and apoptosis. Oncol Rep, Bd 31(Nr. 2):788–794
41. Chiu JJ, Wung BS, Hsieh HJ, Lo LW, Wang DL (2015) Nitric oxide regulates shear stress−induced early growth response-1 expression vipdf. Circ Res 1999(85):238–246
42. Giraldo A et al (2012) Feedback regulation by Atf3 in the endothelin-1-responsive transcriptome of cardiomyocytes: Egr1 is a principal Atf3 target. Biochem J, Bd 444(Nr. 2):343–355
43. Boengler K, Hilfiker-Kleiner D, Heusch G, Schulz R (2010) Inhibition of permeability transition pore opening by mitochondrial STAT3 and its role in myocardial ischemia/reperfusion. Basic Res Cardiol, Bd 105(Nr. 6):771–785
44. Krause MM et al (2003) Nonsteroidal antiinflammatory drugs and a selective cyclooxygenase 2 inhibitor uncouple mitochondria in intact cells. Arthritis Rheum, Bd 48(Nr. 5):1438–1444
45. Crompton M (1999) The mitochondrial permeability transition pore and its role in cell death. Biochem J, Bd 341(Pt 2):233–249
46. Rasola A, Sciacovelli M, Pantic B, Bernardi P (2010) Signal transduction to the permeability transition pore. FEBS Lett, Bd 584(Nr. 10):1989–1996
47. Soldani C, Scovassi AI (2002) Poly ( ADP-ribose ) polymerase-1 cleavage during apoptosis: an update cell death mechanisms: necrosis and apoptosis. Apoptosis, Bd 7(Nr. 4):321–328
48. Gramaglia D et al (2004) Apoptosis to necrosis switching downstream of apoptosome formation requires inhibition of both glycolysis and oxidative phosphorylation in a BCL-X(L)- and PKB/AKT-independent fashion. Cell Death Differ, Bd 11(Nr. 3):342–353
49. Saavedra JE (2001) The secondary amine/nitric oxide complex ion R2N[N(O)NO]- as nucleophile and leaving group in SNAr reactions. J Org Chem 9:10–13
50. Tallarida R (2002) The interaction index: a measure of drug synergism. Pain, Bd 98(Nr. 1–2):163–168